JOURNAL OF MATERIALS SCIENCE 25 (1990) 107-112

Characterization of semiconducting properties of naturally occurring polycrystalline FeS_2 (Pyrite)

S. B. LALVANI*, A. WESTON* and J. T. MASDEN‡
*Mechanical Engineering and Energy Processes, and ‡Department of Physics, Southern Illinois University – Carbondale, Carbondale, Illinois 62901, USA

Naturally occurring polycrystals obtained from Spain and Peru were found to be n-type semiconductors. Samples were characterized using an energy dispersive X-ray analyser and the impurity content of pyrite was estimated. Resistivity and Hall mobility as a function of temperature were measured. A lattice scattering mechanism is found to be operative for the Spanish pyrite sample. Results on optical absorption studies and the crystal structure are also included.

1. Introduction

Pyrite, a naturally occurring semiconductor, is a member of the dichalcogenide family. Pyrite finds its application in the development of FeS_2 electrodes in high-temperature Li–FeS_2 cells [1]. Recent investigations have shown that pyrite can be used as a semiconducting electrode in a photoelectrochemical cell for converting solar into electrical energy [2–4]. This semiconductor material consists of cheap, abundant, non-toxic elements. Several authors have studied solid-state properties of pyrite, using both natural and synthetic samples [5–12]. Pyrite, often present as an impurity in coal, plays a significant role in coal cleaning, utilization and processing.

Pyrite crystallizes in the simple cubic system with iron as Fe^{2+} and sulphur as S_2^{-2} [13]. The most recent pyrite characterization studies indicate that natural crystals have a bandgap energy of about 0.9 eV, while synthetic polycrystals and single crystals have bandgaps of about 0.95 eV [2, 4]. At the valence band, a sulphur 3p character is predominant and overlaps an iron t_{2g} level. The empty conduction band is mainly composed of iron e_g character with some sulphur 3p mixing [4]. Optical transitions across the bandgap occur between quasi-nonbonding bands obtained from donor levels which are present within the bandgap (n-type pyrite) and constitute the upper edge of the valence band.

Marinace [5] found that naturally occurring pyrite is present both as n- as well as p-type semiconductors. Echarri and Sanchez [9] studied natural single crystals of pyrite from Spanish mines which they found to be n-type semiconductors. They studied resistivity, Hall coefficient and mobility as a function of temperature. They observed that an acoustic phonon scattering mechanism is operative in the neighbourhood of room temperatures. Horita [8], in his studies on a Japanese pyrite sample, found that neither acoustic phonon nor impurity scattering are predominant; but he suggested that a hopping type conduction or scatterings by ionized impurities with deep energy levels may be operative.

The objective of this research was to systematically investigate the Hall effect, resistivity and optical behaviour of two diverse n-type naturally occurring pyrites of known compositions.

2. Experimental details

Pyrite samples were obtained from the Wards National Science Establishment, (Rochester, New York). Sample 8 is an n-type semiconductor from Muro de Aguas, Ambassaguas, Navarre Mountains, Spain while Sample 2 comes from Peru. The samples were cut of natural crystals, a diamond disc and diamond wire saw were used for this purpose. Water was the sole lubricant used in order to reduce the amount of unnecessary contaminants. Prior to the measurements of electrical properties, the samples were etched with a mixture of H_2O_2 (30 wt %)–HCl (38 wt %) (1:1 volume ratio) under potentiostatic conditions.

3. Results and discussion

3.1. Elemental analysis and crystal structure

A scanning electron microscope with an energy dispersive X-ray analyser was used to study the surface of Sample 8 pyrite. Pyrite sample ($< 1\,\mu m$) was subjected to X-rays generated at an accelerating voltage of 20 KeV. The results obtained are presented in Table I. The atomic weight per cent analysis indicates that Sample 8 can be represented chemically as FeS_2. No significant extent of segregation of either iron or sulphur was found. It must be however noted that during our analysis, grains of aluminium and silicon were found in significant quantities at the surface of the sample.

Pyrite samples were also analysed for trace element composition. Samples were just subjected to a HNO_3 wash at 25° C. The solution was then

0022-2461/90 $03.00 + .12

TABLE I Elemental analysis of Sample 8

Element	Weight (%)	Atomic weight (%)
S	53.53	67.13
Fe	45.83	32.87

$\frac{S}{Fe}$ (atomic ratio) = 2.04

diluted with distilled water (1:1 volume ratio). The assays were analysed by atomic absorption for ten elements: Al, Ca, Co, Cu, Mg, Ni, Ti, Si and Zn. The results (Table II) indicate that a significant variety of impurities are present in the naturally occurring pyrite samples. For example, Sample 8 has a large Al, Si, Co, Mg, Ni and Ca content while Sample 2 has relatively low impurity content. These impurities impart "metal-like" behaviour to pyrite as evidenced by the data presented elsewhere in this paper.

Sample 8 was ground to powder and analysed by X-ray diffraction by means of a General Electric powder diffraction camera with copper radiation (λ = 0.154 34 nm). The X-ray was powdered with 30 kV and 25 mA d.c. The results indicate that the structure of Sample 8 is simple cubic, which contrasts with the face centred cubic structure known to be common to pyrite [2]. The lattice parameter obtained was 0.5397 nm.

3.2. Hall effect measurements

Hall effect experiments on Sample 8 were conducted at 25 to 50° C in a 4.5 kG Magnetic field. The experiment requires a uniform magnetic field applied perpendicular to the face of a sample wafer. A set current was applied through two opposing ends of the rectangular wafer and the Hall voltage across the other two ends was recorded accordingly. Hall voltages of up to -100 V were observed, the negative direction of the voltage confirmed the fact that Sample 8 is an n-type semiconductor. Calculated values of the Hall coefficient are plotted against current (Fig. 1). The results indicate that the Hall coefficient remains fairly constant for the temperature range considered. Studies undertaken by Echarri and Sanchez [9] show little variation in the Hall coefficient for temperature ranging from -190 to 60° C. The extrapolated value at zero current yields the true Hall coefficient which can be used to calculate electron and hole mobility. The extrapolated Hall coefficient value for Sample 8 is about 0.038 cm^3 C^{-1}. This yields a majority current charge carrier concentration of 1.6×10^{20} cm^{-3} which is high for semiconductor and approaches metal carrier concentration.

TABLE II Trace element composition of Samples 8 and 2

Element	Sample 8 concentration (ppm)	Sample 2 concentration (ppm)
Al	59.75	3.89
Ca	78.37	21.77
Co	14.87	1.06
Cu	1.79	4.02
Mg	19.27	8.17
Na	7.89	8.78
Ni	26.25	5.81
Ti	0.05	B.D.*
Si	47.85	29.82
Zn	7.71	8.96

*B.D. : Below Detection limits (about 0.005 ppm)

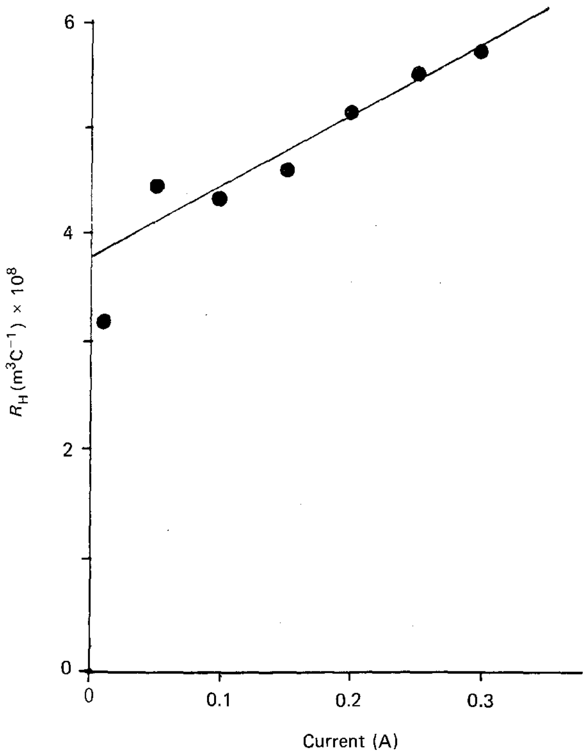

Figure 1 Hall coefficient plotted against bias current for (Sample 8) at 25° C.

The temperature dependence of mobility was also determined (Fig. 2). At high temperature, mobility is observed to be proportional to $T^{-1.46}$. This temperature dependence is characteristic of lattice scattering mechanism (typical temperature dependence: $T^{-1.5}$) where carriers moving through the lattice encounter atoms which are out of their normal lattice positions due to thermal vibration. These observations are in agreement with the findings of Echarri and Sanchez [9]. However, it must be noted that Horita [8] suggested that a hopping type conduction mechanism may be responsible for the observed behaviour of a Japanese pyrite.

3.3. Resistivity measurements

The temperature dependence of the resistivity of pyrite samples was measured from ambient temperature to 100° C and then down to liquid nitrogen temperatures reaching -190° C. The data indicate that Sample 2 has resistivities of the order of 10 to 70 Ω cm for the temperature interval considered while Sample 8 has corresponding values for resistivity which are three orders of magnitude lower (90 to 20 mΩ cm) (Figs 3 and 4). The resistivity of Sample 8 increases with temperature, while it generally decreases with temperature for Sample 2. In a narrow range of temperature (-115 to -150° C), the resistivity is found to be independent of temperature for Sample 2. This transition region is inherent to doped semiconductors, as it represents a break between electron and hole mobility due to impurity or lattice scattering. For an

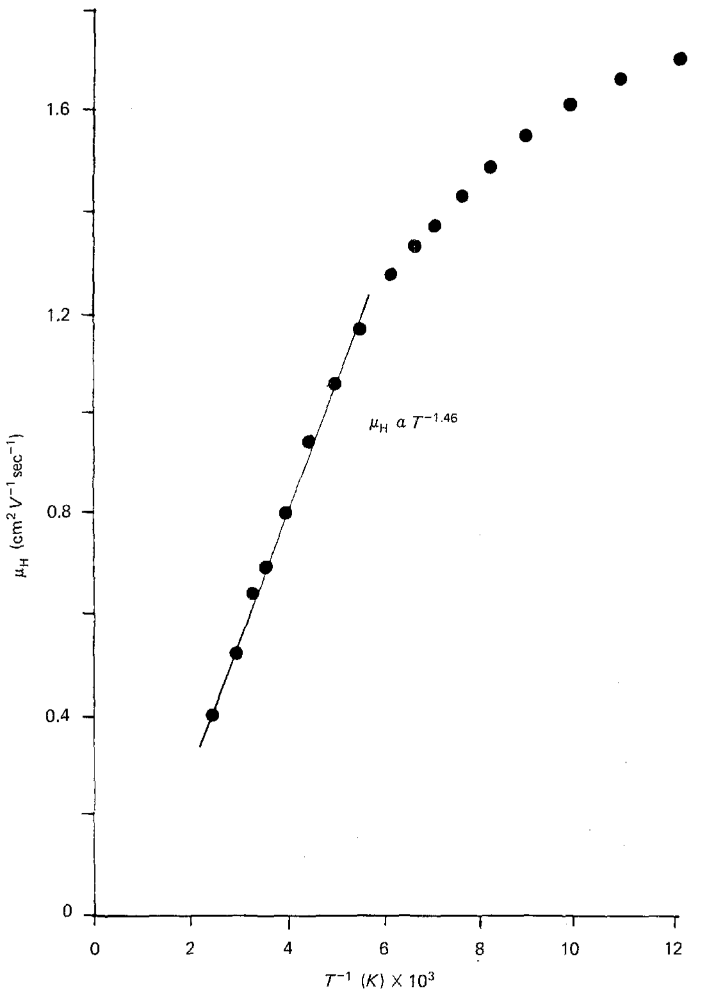

Figure 2 Current mobility plotted against temperature (Sample 8).

n-type semiconductor, at low temperatures donor electrons are bound to atoms and as temperature increases, these electrons are donated to the conduction band (ionization band). This occurs until all donor atoms are ionized (extrinsic regime) and is represented by the transition in the resistivity data for Sample 2. At higher temperatures intrinsic carriers dominate (intrinsic regime). The behaviour of Sample 8 is more metallic in nature.

From the intrinsic region in Fig. 3, the energy gap E_g is estimated to be about 0.22 eV in the temperature interval of 0 to 100° C using the approximate relation $\varrho \alpha \exp (E_g/2kT)$. While, various values have been reported: 0.73 to 1.2 eV for the energy gap (5 to 8) these values are estimated by the same approximations as described above. However, the absorption method (see next section) yields a band gap value of about 0.87 eV at room temperature.

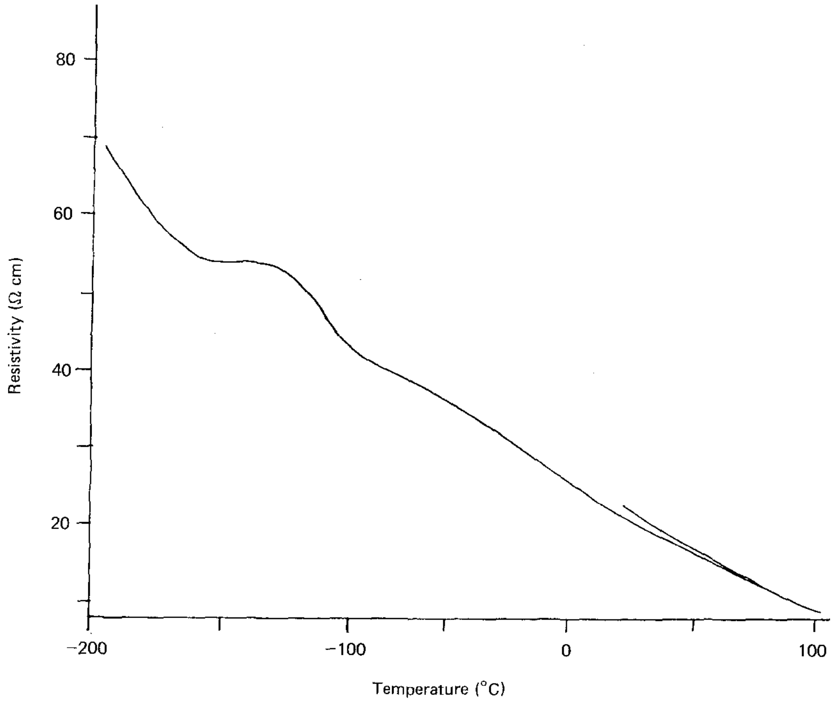

Figure 3 Resistivity plotted against temperature (Sample 2).

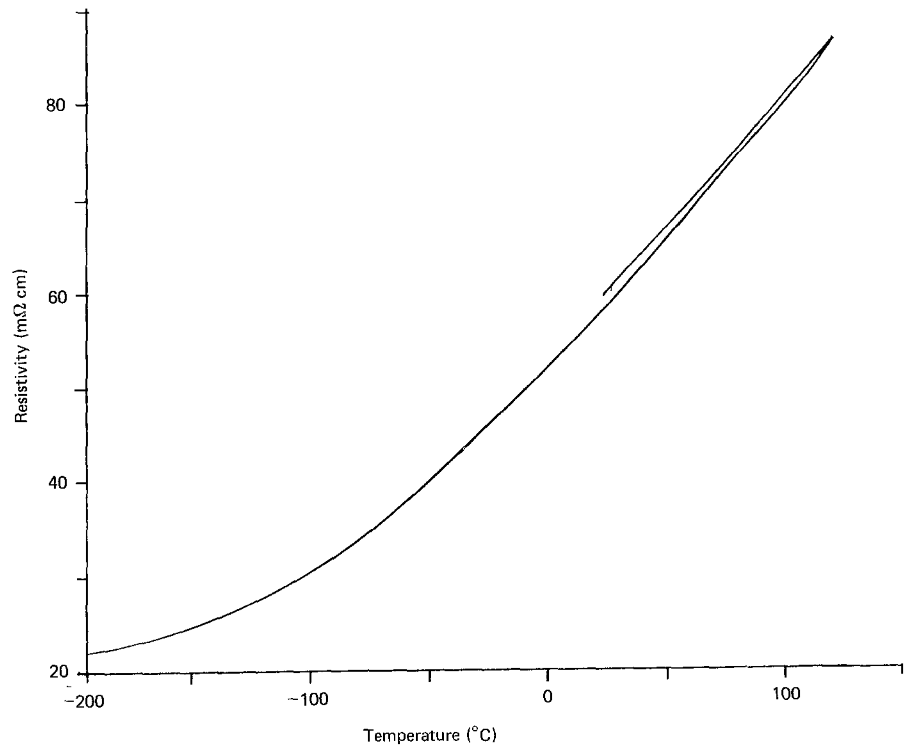

Figure 4 Resistivity plotted against temperature (Sample 8).

3.4. Optical absorptivity measurements

The pyrite samples were sliced and attached to a quartz plate using clear epoxy resin. The platelets were then polished with silicon carbide abrasive pads and etched with HF–CH_3COOH–HNO_3. Photons at different wavelengths were directed at the pyrite samples and the corresponding transmission of photons through the samples was recorded. Photons with energies greater than the band gap are absorbed, those with lower energies are transmitted. The absorptivity of the sample was obtained using the following physical relationship

$$I_t = I_0 \exp(-\alpha t)$$

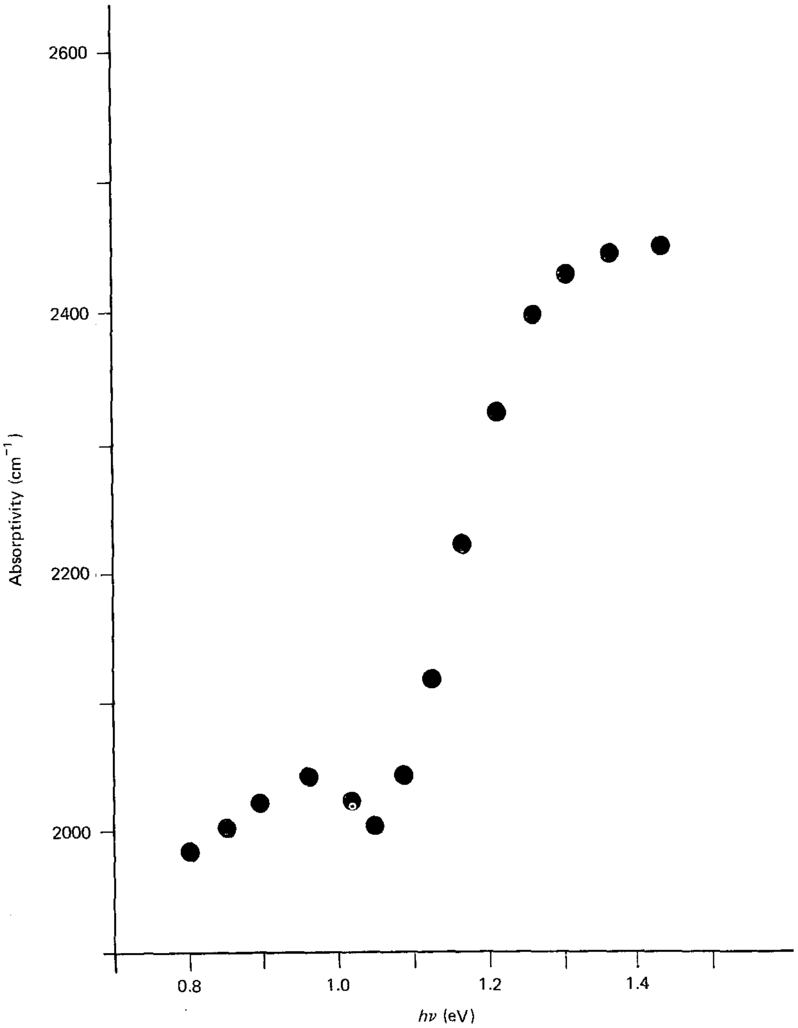

Figure 5 Absorptivity plotted against photon energy.

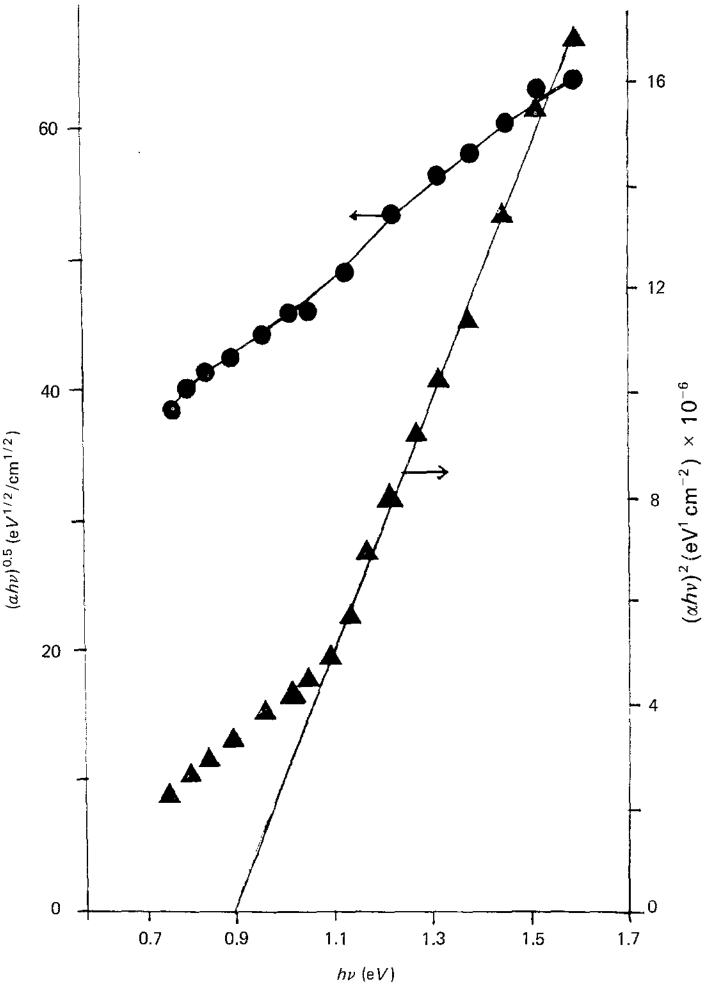

Figure 6 $(\alpha h\nu)^{n/2}$ plotted against photon energy.

where I_t and I_0 are, respectively, the transmitted and incident light intensities, α the absorption coefficient and t the sample thickness.

Characteristic absorptivity values for pyrite range from 2850 cm^{-1} at 1.60 eV to 1620 cm^{-1} at 0.77 eV. From the plot of absorptivity against photon energy (Fig. 5) for Sample 8, it can be readily seen that a transition occurs around 1.1 eV (1130 nm) and absorptivity increases to a maximum. These absorptivity values correspond to an optical absorption depth (α^{-1}) of the order of 390 to 620 μm. The band gap of a semiconductor can be estimated by employing the following equation

$$\alpha = \frac{A\,(h\nu - E_g)^{n/2}}{h\nu}$$

where $n = 1$ and 4 are respectively for direct and indirect band gap semiconductor. A plot of the above equation (Fig. 6) indicates that the pyrite Sample 8 examined in the study is a direct band gap semiconductor with a band gap value of about 0.87 eV. The optical absorption edge ($n = 2$) corresponds to the threshold for electron transfer between the highest nearly filled band and the lowest nearly empty band. The optical absorption edge for Sample 8 was obtained by extrapolating the plot of ($\alpha h\nu$) against $h\nu$ and it was found to be equal to 0.94 eV.

4. Comments

The data obtained indicate a large discrepancy between the energy gap deduced from the Hall–resistivity studies and that from the absorption studies. The following explanation is offered for this anomaly. Pyrite, although a semiconductor has some metallic character as well. Resistivity changes are attributed to different phenomena according to the metal–semiconductor behaviour of materials. For metals the number of charge carriers is approximately constant while any change in mobility results in a corresponding change in resistivity. On the other hand in semiconductors, the mobility of charge carriers is approximately constant while a change in the number of carrriers results in a corresponding change in resistivity. In order to test whether the samples used in this study lie in some intermediate metal–semiconductor range where the contribution to resistivity changes due to both mobility and the number of carriers is significant, the following analysis was conducted. A plot of log of resistivity times mobility against the reciprocal of temperature was prepared which yielded a band gap value of 0.31 eV. This band gap value is about 41% higher than the corresponding value (of 0.22 eV) obtained from the resistivity against temperature data. Thus one may conclude that the mobility temperature dependence does contribute to provide a higher value of E_g but this value is still lower than that (0.87 eV) obtained from the absorption data.

The pyrite samples have a large carrier concentration of about 1.6×10^{20} which could induce a donor level close to the conduction band. This donor level may have been the most significant contributor to the resistivity–band gap estimation. It seems that the electrical technique in comparison to the absorption studies for estimating band gap, is more sensitive (or possibly "excites") to the donor levels. In the latter case when excited the electrons jump from the valence to the conduction band directly thus resulting in higher values for E_g.

5. Conclusions

Impurities can impart "metal-like" behaviour to the naturally occurring pyrite semiconductor. A lattice scattering mechanism is found to be operative for the Spanish pyrite sample in this study. A comparison of our results including the elemental analysis and crystal structure with the published data suggests that naturally occurring pyrite samples do not display uniform properties. It is suspected that to a large extent impurities present determine the physical behaviour of pyrite samples.

Acknowledgement

The financial support provided by the Department of Energy and the Illinois Mines and Minerals Resources Research Institute is gratefully acknowledged.

References

1. T. D. KAUN, *J. Electrochem. Soc.* **132** (1985) 3063.
2. W. JAEGERMANN, and H. TRIBUTSH, *J. Appl. Electrochem.* **13** (1983) 743–750.
3. A. ENNAOUI and H. TRIBUTSH, *Solarcells* **13** (1984) 197–200.
4. A. ENNAOUI, W. JAEGERMANN, and H. TRIBUTSH, *J. Electrochem. Soc.* **133** (1986) 97–106.
5. J. C. MARINACE, *Phys. Rev.* **57** (1954) 593.
6. T. A. BITHER, R. J. BOUCHARD, W. H. CLOUD, P. C. DONOHUE and W. J. SIEMONS, *Inorg. Chem.* **7** (1968) 2208.
7. E. K. LI, K. H. JOHNSON, D. E. EASTMAN and J. L. FREEOUF, *Phys. Rev. Lett.* **32** (1974) 470.
8. H. HORITA, *Jpn J. Appl. Phys.* **12** (1973) 617–618.
9. A. L. ECHARRI and C. SANCHEZ *Solid State Commun.* **15** (1974) 827–831.
10. A. SCHLEGEL and P. WACHTER, *J. Phys. C.* **9** (1976) 3363.
11. M. A. KHAN, *ibid.* **9** (1976) 81.
12. Ch. SUGIURA, *J. Chem. Phys.* **80** (1984) 1047.
13. R. T. SHUEY, "Semiconducting Ore Minerals", (Elsevier, London, 1975). pp. 304–309.

Received 3 February 1988
and accepted 14 April 1989